

Article

Investigation of Lupeol as Anti-Melanoma Agent: An In Vitro-In Ovo Perspective

Flavia Bociort ^{1,†}, Ioana Gabriela Macasoï ^{2,3,†}, Iasmina Marcovici ^{2,3,*}, Andrei Motoc ¹, Cristina Grosu ², Iulia Pinzaru ^{2,3} , Crina Petean ², Stefana Avram ^{2,3}  and Cristina Adriana Dehelean ^{2,3}

¹ Faculty of Medicine, “Victor Babes” University of Medicine and Pharmacy Timisoara, Eftimie Murgu Square No. 2, 300041 Timisoara, Romania; flavia.bociort@umft.ro (F.B.); amotoc@umft.ro (A.M.)

² Faculty of Pharmacy, “Victor Babes” University of Medicine and Pharmacy Timisoara, Eftimie Murgu Square No. 2, 300041 Timisoara, Romania; macasoï.ioana@umft.ro (I.G.M.); cristina.grosu@umft.ro (C.G.); iuliapinzaru@umft.ro (I.P.); crina.petean@umft.ro (C.P.); stefana.avram@umft.ro (S.A.); cadehelean@umft.ro (C.A.D.)

³ Research Center for Pharmaco-Toxicological Evaluations, “Victor Babes” University of Medicine and Pharmacy Timisoara, Eftimie Murgu Square No. 2, 300041 Timisoara, Romania

* Correspondence: iasmina.marcovici@umft.ro; Tel.: +40-763-734-139

† These authors contributed equally to this work.

Abstract: Malignant melanoma (MM) represents the most life-threatening skin cancer worldwide, with a narrow and inefficient chemotherapeutic arsenal available in advanced disease stages. Lupeol (LUP) is a triterpenoid-type phytochemical possessing a broad spectrum of pharmacological properties, including a potent anticancer effect against several neoplasms (e.g., colorectal, lung, and liver). However, its potential as an anti-melanoma agent has been investigated to a lesser extent. The current study focused on exploring the impact of LUP against two human MM cell lines (A375 and RPMI-7951) in terms of cell viability, confluence, morphology, cytoskeletal distribution, nuclear aspect, and migration. Additionally, the in ovo antiangiogenic effect has been also examined. The in vitro results indicated concentration-dependent and selective cytotoxicity against both MM cell lines, with estimated IC₅₀ values of 66.59 ± 2.20 for A375, and 45.54 ± 1.48 for RPMI-7951, respectively, accompanied by a reduced cell confluence, apoptosis-specific nuclear features, reorganization of cytoskeletal components, and inhibited cell migration. In ovo, LUP interfered with the process of angiogenesis by reducing the formation of neovascularization. Despite the potential anti-melanoma effect illustrated in our in vitro-in ovo study, further investigations are required to elucidate the underlying LUP-induced effects in A375 and RPMI-7951 MM cells.

Keywords: lupeol; skin cancer; malignant melanoma cells; angiogenesis



Citation: Bociort, F.; Macasoï, I.G.; Marcovici, I.; Motoc, A.; Grosu, C.; Pinzaru, I.; Petean, C.; Avram, S.; Dehelean, C.A. Investigation of Lupeol as Anti-Melanoma Agent: An In Vitro-In Ovo Perspective. *Curr. Oncol.* **2021**, *28*, 5054–5066. <https://doi.org/10.3390/curroncol28060425>

Received: 11 October 2021

Accepted: 1 December 2021

Published: 2 December 2021

Publisher’s Note: MDPI stays neutral with regard to jurisdictional claims in published maps and institutional affiliations.



Copyright: © 2021 by the authors. Licensee MDPI, Basel, Switzerland. This article is an open access article distributed under the terms and conditions of the Creative Commons Attribution (CC BY) license (<https://creativecommons.org/licenses/by/4.0/>).

1. Introduction

Malignant melanoma (MM) is described as the tumor arising from the neoplastic transformation of melanin-producing cells—the melanocytes [1], and the leading cause of skin cancer-related deaths worldwide [2] despite its rareness [3]. The pathogenesis of MM is multifactorial [4]. However, cutaneous MM (CMM) development is primarily the consequence of skin exposure to environmental carcinogens, such as ultraviolet radiation (UVR) from natural or artificial sources [3]. Other noxious factors leading to CMM occurrence include gene mutations (e.g., CDKN2A, p53, RB1, BRAF), immunosuppression, oxidative stress due to reactive oxygen species (ROS) generation, and inflammatory responses [4,5]. Treatment strategies vary from surgical resection to chemo-, radio-, and immuno-therapies, being highly dependent on the tumor stage, location, and genetics. Chemotherapy (e.g., dacarbazine) was the first-line option for advanced melanoma management [6–8], but due to severe adverse events, drug resistance, and lack of survival benefit, the treatment success rate has been considerably lowered [9–11]. The management of metastatic MM has

significantly progressed with the emergence of targeted therapy and immune checkpoint inhibitors. However, each therapy option presents several limitations. Targeted therapy (e.g., vemurafenib, dabrafenib) has been associated with a high response rate, but also with short-term therapeutic benefits and rapid development of tumor resistance (within several months). Conversely, the treatment with immune checkpoint inhibitors (e.g., ipilimumab, pembrolizumab, nivolumab, atezolizumab) generates a superior overall survival among patients, but a lower response rate [11,12]. To overcome the current difficulties enquired in the treatment of advanced MM, improved therapeutic strategies are deeply required.

Medicinal plants serve as excellent sources for drug discovery and development due to their richness in secondary metabolites displaying a wide structural and pharmacological diversity that favors this process [13]. Natural compounds are extensively investigated as complementary or alternative choices in cancer prevention or chemotherapy [14]. In regard to MM, plant constituents (e.g., terpenoids, flavonoids) [7,15] generally serve as potent anti-melanoma agents by inhibiting the proliferation, migration, and metastasis of melanoma cells [9]. Lupeol (LUP) is a dietary pentacyclic lupane-type triterpenoid found in various foods, such as fruits and vegetables, as well as medicinal plants. From a therapeutic point of view, the latest research of the pharmacological properties of LUP suggests a broad portfolio of biological effects, such as antioxidant, anti-inflammatory, antimicrobial, and skin protective [16,17]. In addition, the anticancer activity of LUP has been demonstrated against several malignancies, such as colorectal, lung, and liver neoplasms [18–20]. However, the data on the potential of LUP in malignant melanoma treatment remain scarce.

The current study aims at providing an *in vitro-in ovo* insight into the anti-proliferative, anti-metastatic, and antiangiogenic properties of LUP as a potential chemotherapeutic agent in malignant melanoma management.

2. Materials and Methods

2.1. Reagents

Lupeol, trypsin-EDTA solution, phosphate saline buffer (PBS), dimethyl sulfoxide (DMSO), fetal calf serum (FCS), penicillin/streptomycin, and MTT [3-(4,5-dimethylthiazol-2-yl)-2,5-diphenyltetrazolium bromide] reagent were purchased from Sigma Aldrich, Merck KgaA (Darmstadt, Germany). The cell culture media, Dulbecco's Modified Eagle Medium (DMEM; ATCC® 30-2002™) and Eagle's Minimum Essential Medium (EMEM; ATCC® 30-2003™), were purchased from ATCC (American Type Cell Collection, Lomianki, Poland). Hoechst 33342 reagent was obtained from Invitrogen by Thermo Fisher Scientific (Waltham, MA, USA). All reagents were analytically pure and proper for cell culture use.

2.2. Cell Culture

The anti-melanoma effect of LUP was evaluated on two human MM cell lines provided by ATCC as frozen vials—A375 (CRL-1619™), and RPMI-7951 (HTB-66™). The biosafety of LUP was assessed on two healthy skin cell types (human keratinocytes—HaCaT, and human fibroblasts—1BR3) provided as frozen vials by CLS Cell Lines Service GmbH (Eppelheim, Germany), and the European Collection of Authenticated Cell Cultures (ECACC, Salisbury, UK), respectively. Each cell line was cultured in its specific growth medium (A375 and HaCaT in DMEM, and RPMI-7951 in EMEM) containing 10% FCS and 1% penicillin (100 U/mL)-streptomycin (100 µg/mL) mixture. The 1BR3 cells were cultured in EMEM medium supplemented with 15% FCS and antibiotics. The cells were incubated in standard conditions (37 °C, and 5% CO₂) during the experiments.

2.3. Cellular Viability and Morphology Assessment

The cell viability was assessed by applying the MTT technique. Briefly, A375, RPMI-7951, HaCaT, and 1BR3 cells were cultured in 96-well plates (10⁴ cells/well) and stimulated with five concentrations (10, 20, 30, 40, and 50 µM) of LUP. DMSO was used for the preparation of the LUP stock solution. After 24 h of treatment, fresh media (100 µL) and MTT

reagent (10 μ L) were added in each well, and the plates were incubated for 3 h at 37 °C. The final steps included: addition of the solubilization solution (100 μ L/well), incubation of the plates at room temperature for 30 min, protected from light, and absorbance measurement at two wavelengths (570 and 630 nm) using Cytation 5 (BioTek Instruments Inc., Winooski, VT, USA). In order to verify the potential impact of LUP on A375 and RPMI-7951 cells' morphology and confluence, a microscopic evaluation was performed by photographing the cells under bright field illumination at the end of the 24 h stimulation period using Cytation 1 (BioTek Instruments Inc., Winooski, VT, USA). The pictures were analyzed using the Gen5™ Microplate Data Collection and Analysis Software (BioTek Instruments Inc., Winooski, VT, USA).

2.4. Nuclear Morphology Evaluation

To evaluate the potential toxicity of LUP at the nuclear level, Hoechst 33342 staining was applied according to the manufacturer's recommendations. In brief, the A375 and RPMI-7951 cells were seeded in 12-well plates (10⁵ cells/well) and treated with three increasing concentrations (10, 30, and 50 μ M) of LUP. After 24 h, the media was removed, the staining solution (1:2000 dilution in PBS) was added (500 μ L/well), and the plates were incubated, protected from light, at room temperature, for 10 min. Finally, the cells were washed with PBS, photographed using Cytation 1 (BioTek Instruments Inc., Winooski, VT, USA), and analyzed using Gen5™ Microplate Data Collection and Analysis Software (BioTek Instruments Inc., Winooski, VT, USA).

2.5. Immunofluorescence

For the immunofluorescent visualization of the cellular components, A375 and RPMI-7951 cells (10⁵ cells/well) were seeded in 12-well plates and stimulated with LUP (10, 30, and 50 μ M). After 24 h, the cells were washed with ice-cold PBS, fixed with paraformaldehyde 4% for 1 h at room temperature (RT), and permeabilized with a Triton X/PBS 2% for 30 min at RT, followed by a blocking step with 30% FBS in 0.01% Triton X for 1 h. The actin fibers (AF) were highlighted using Alexa Fluor® 555 Phalloidin antibody (Cell Signaling Technology, Danvers, MA, USA) (overnight incubation at 4 °C). For the staining of microtubules (MTs), the cells were incubated overnight with the primary antibody (α -tubulin antibody, Invitrogen by Thermo Fisher Scientific) in a dark humidity chamber at 4 °C, followed by an incubation (dark humidity chamber, 4 °C, 1 h) with a fluorescent-labeled (Alexa Flour™ 488, Invitrogen by Thermo Fisher Scientific) goat anti-rabbit secondary antibody, the next day. The final step consisted of the counterstaining of the cells' nuclei with 40,6-diamidino-2-phenylindol (DAPI) for 15 min.

2.6. Wound Healing Assay

The influence of LUP on the metastatic character of A375 and RPMI-7951 cells was evaluated by applying the wound healing (scratch) assay. In summary, the cells (10⁵ cells/1 mL/well) were cultured in 24-well Corning plates, and an automatic scratch was made in the middle of each well using the AutoScratch™ Wound Making Tool provided by BioTek® Instruments Inc., Winooski, VT, USA as recommended by the manufacturer. The cells were treated with the test compound at three concentrations (10, 20, and 30 μ M) for 24 h and representative images (4 \times magnification) were taken at the beginning of the assay (0 h) and at its end (24 h) using Cytation 1 and were processed using Gen5™ Microplate Data Collection and Analysis Software (BioTek® Instruments Inc., Winooski, VT, USA). The quantification of the effect of LUP in terms of cell migration was performed by calculating the migration rates (%) according to a formula by Felice et al. [21] which has been also used in our previous work [22].

2.7. Chorioallantoic Membrane (CAM) Assay

Fertilized chicken eggs were used to determine the potential anti-angiogenic effect. Their preparation consisted of disinfecting the eggs with alcohol of 70% concentration,

dating them, and placing them in an incubator in a vertical position. On the 3rd day of incubation, a volume of 7 mL of albumen was extracted with a syringe in order to promote the detachment of the chorioallantoic membrane from the inner shell of the egg, so that the blood vessels are easier to observe. On the next day of incubation, the 4th day, a window was cut in the horizontal part of the eggs which was subsequently covered with adhesive tape, and the eggs were reintroduced into the incubator until the beginning of the experiment. The study of angiogenesis began on the 7th day of incubation. To highlight the potential antiangiogenic effect of LUP, it was tested at a concentration of 50 μM and blood vessels were observed for a period of 24 h. During this time, angiogenesis shows a rapid rate of development, similar to that observed in angiogenesis in the tumor process [23].

2.8. Statistical Analysis

All data are expressed as means \pm SD, the differences being compared by applying the one-way ANOVA analysis followed by Dunett's multiple comparisons post-test. The used software was GraphPad Prism version 9.2.0 for Windows (GraphPad Software, San Diego, CA, USA). The statistically significant differences between data were labeled with * ($p < 0.1$); ** ($p < 0.01$); *** ($p < 0.001$); **** ($p < 0.0001$).

3. Results

3.1. Cellular Viability and Morphology Assessment

In order to evaluate the potential anti-melanoma effect of LUP, the viability of A375 and RPMI-7951 malignant melanoma cells has been assessed following a 24 h treatment with ascending concentrations (10–50 μM) of LUP. The results indicated a dose-dependent cytotoxic activity of LUP on both cell lines (Figure 1A,B), the highest inhibition of the cell viability being recorded at the highest concentration tested (50 μM) when the percentages reached the values of 61.29% for A375 and 37.78% for RPMI-7951, respectively. Despite the similar viability trend observed in both cell lines, RPMI-7951 cells ($\text{IC}_{50} = 45.54 \pm 1.49$) exerted a higher sensitivity to the anti-tumor effect of LUP as compared to A375 ($\text{IC}_{50} = 66.59 \pm 2.20$). As a component of the in vitro anti-cancer profile of LUP, its impact on the morphology and confluence of A375 and RPMI-7951 melanoma cells has been examined by monitoring and photographing the cells at the end of the 24 h incubation period. The results confirm the concentration-dependent effect of LUP which initiates the loss of cellular confluency at the lowest concentration of 10 μM . The most prominent effect however has been recorded after the cells' treatment with the highest concentration of LUP (50 μM). In addition, cell roundness can be observed at 30 and 50 μM which are consistent with cellular death (Figure 1C). The potential skin toxicity has been assessed using human keratinocytes (HaCaT) and fibroblasts (1BR3). After 24 h of treatment, LUP induced a dose-dependent decline in the viability of HaCaT and 1BR3 cells (Figure 2). The highest viability decrease has been registered at the concentration of 50 μM : 91% for HaCaT, and 93.48% for 1BR3 cells. The estimated IC_{50} values are $210.82 \pm 25.09 \mu\text{M}$ (HaCaT), and $346.25 \pm 12.84 \mu\text{M}$ (1BR3).

3.2. Nuclear Morphology Evaluation

In order to provide a preliminary evaluation on the cytotoxic mechanism of LUP, the cell nuclei were examined in terms of morphological changes by the means of Hoechst 33342 staining. The interpretation of the results has been performed according to a previous publication by Crowley et al. [24]. Staurosporine (STP) 5 μM was used as positive control for this assay and induced significant changes in the aspect of A375 and RPMI-7951 cellular nuclei, such as fragmentation and dysmorphology. Regarding the effect induced by LUP, in A375 cells no significant changes were detected at 10 μM as compared to the control (untreated cells), while at higher concentrations specific apoptotic features (indicated by arrows) can be noticed, such as nuclear fragmentation, and apoptotic bodies (LUP 20 μM), membrane blebbing, and chromatin condensation (LUP 50 μM). In the case of RPMI-7951 cells, signs of apoptosis (membrane blebbing, fragmentation of cellular nuclei) have been recorded at all concentrations (indicated by arrows). The results are presented in Figure 3.

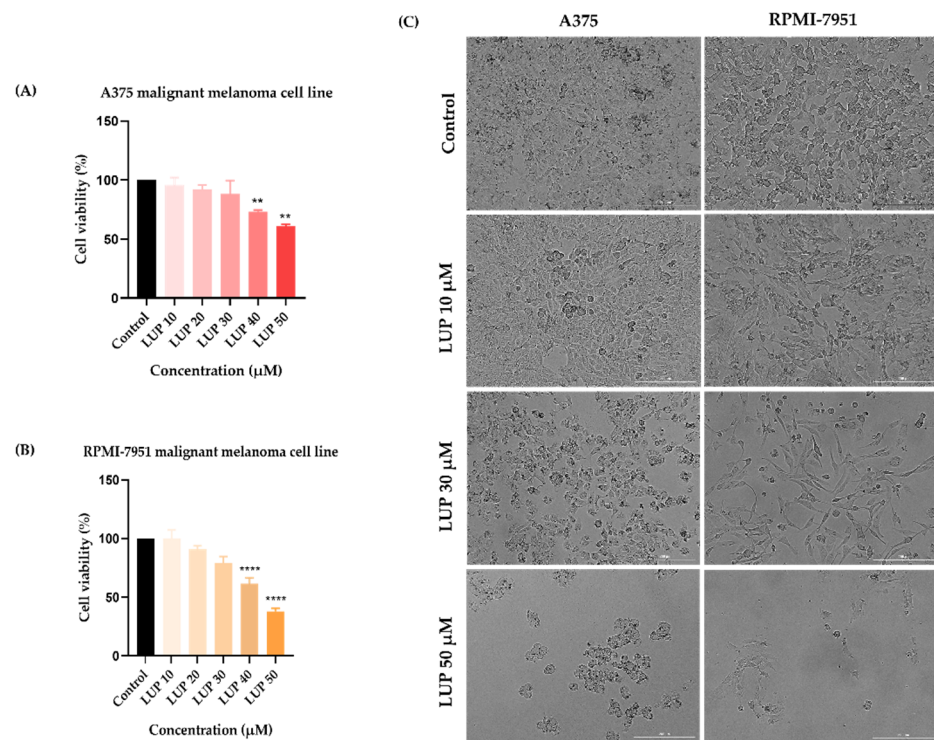


Figure 1. In vitro assessment of the effect LUP (10, 20, 30, 40 and 50 μM) exerts on the viability of (A) A375 and (B) RPMI-7951 MM cells after 24 h of treatment by applying the MTT assay and (C) morphology and confluence of A375 and RPMI-7951 MM cells following the 24 h treatment with LUP 10, 30, and 50 μM. The data are expressed as viability percentages (%) normalized to control cells and expressed as mean values ± SD of three independent experiments performed in triplicate. To identify the statistical differences between the control and the LUP-treated group, a one-way ANOVA analysis was conducted followed by the Dunett’s multiple comparisons post-test (** $p < 0.01$; **** $p < 0.0001$). The image scale bars indicate 200 μm.

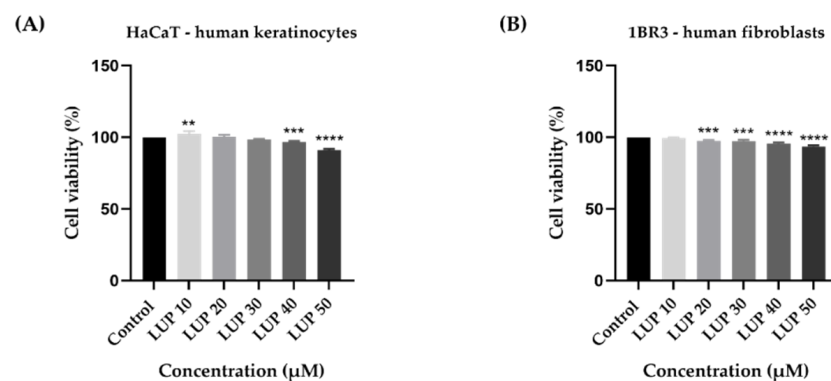


Figure 2. In vitro assessment of the effect LUP (10, 20, 30, 40 and 50 μM) exerts on the viability of (A) HaCaT and (B) 1BR3 healthy skin cells after 24 h of treatment by applying the MTT assay. The data are expressed as viability percentages (%) normalized to control cells and expressed as mean values ± SD of three independent experiments performed in triplicate. To identify the statistical differences between the control and the LUP-treated group, a one-way ANOVA analysis was conducted followed by the Dunett’s multiple comparisons post-test (** $p < 0.01$; *** $p < 0.001$; **** $p < 0.0001$).

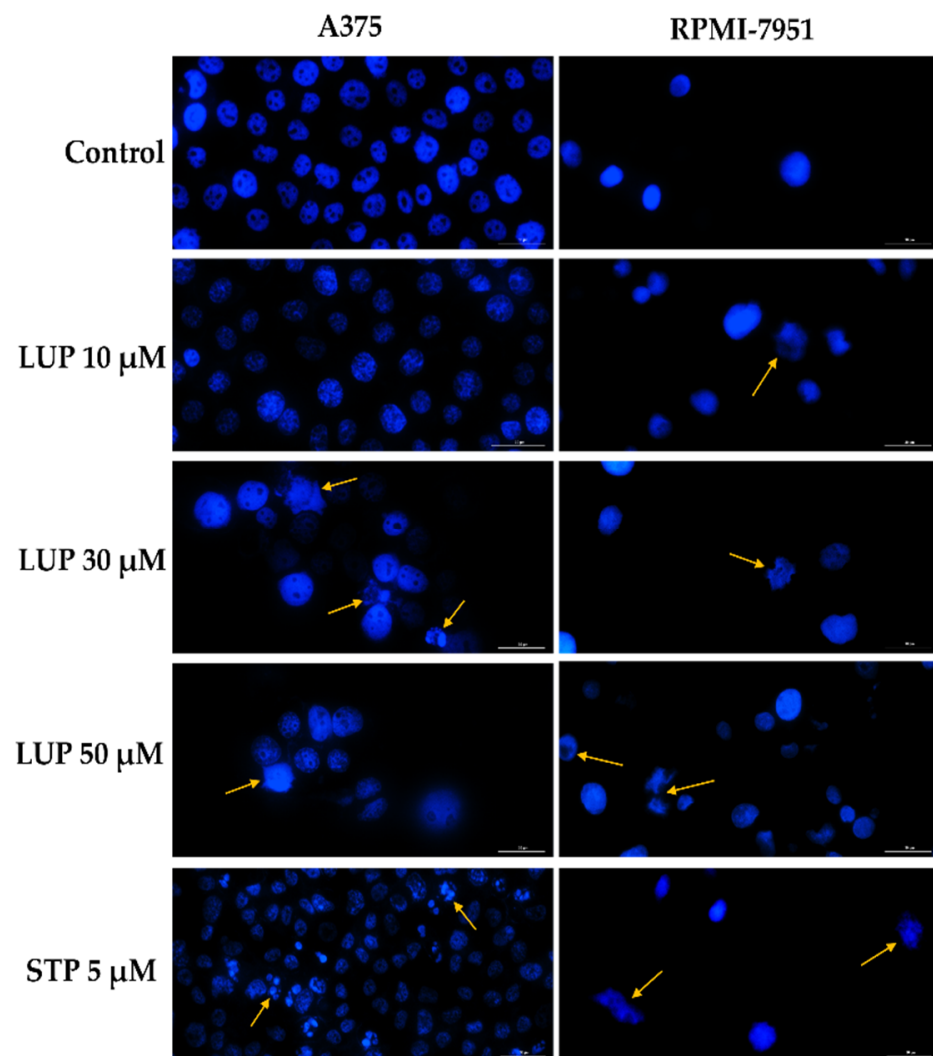


Figure 3. Cell nuclei staining using Hoechst 33342 in A375 and RPMI-7951 malignant melanoma cells following the 24 h treatment with LUP 10, 30, and 50 μM . Staurosporine (STP) 5 μM was selected as positive control for apoptosis. The arrows indicate apoptotic nuclei expressing specific features. The scale bars represent 30 μm .

3.3. Immunofluorescence

To obtain a complete insight into the impact of LUP on the morphology of A375 and RPMI-7951 melanoma cells, a fluorescence immunochemistry technique has been applied highlighting the changes that occurred within the distribution of cytoskeletal components (actin filaments—red, and microtubules—green) following the 24 h treatment. In addition, the cell nuclei were counterstained with DAPI. At the lowest concentration tested (10 μM) LUP induced no significant changes in the aspect of the A375 and RPMI-7951 cells' cytoskeleton. However, at higher concentrations (30 and 50 μM), several changes in the AF and MTs organization can be observed (indicated by arrows) as follows: (i) in A375 cells (Figure 4)—condensation of actin bundles and reorganization of MTs into a cortical ring leading to cell rounding; and (ii) in RPMI-7951 cells (Figure 5)—actin condensation, perinuclear distribution of MTs, and reduced length of the cells' longitudinal axis.

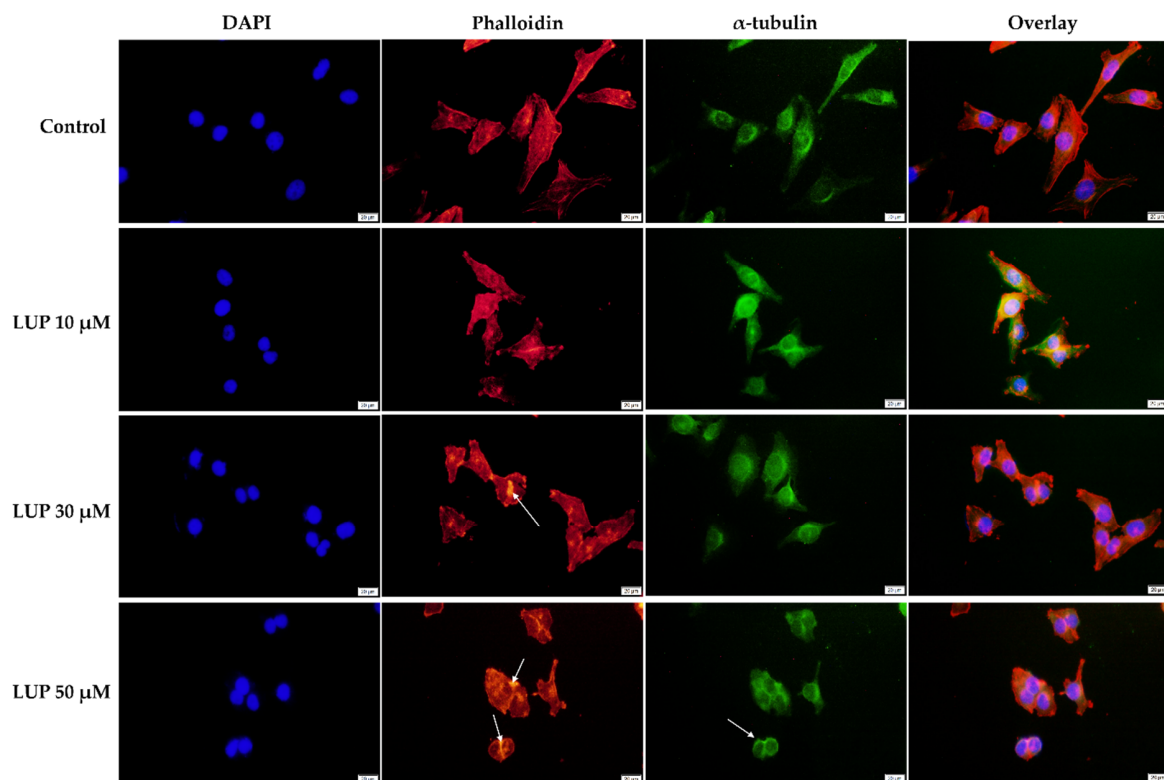


Figure 4. Human melanoma cells (A375) visualized by fluorescence microscopy following the 24 h treatment with LUP (10, 30, and 50 μM). Cell nuclei (DAPI), actin filaments (phalloidin), and microtubules (α -tubulin) are presented individually and also combined (overlay). The scale bars indicate 20 μm .

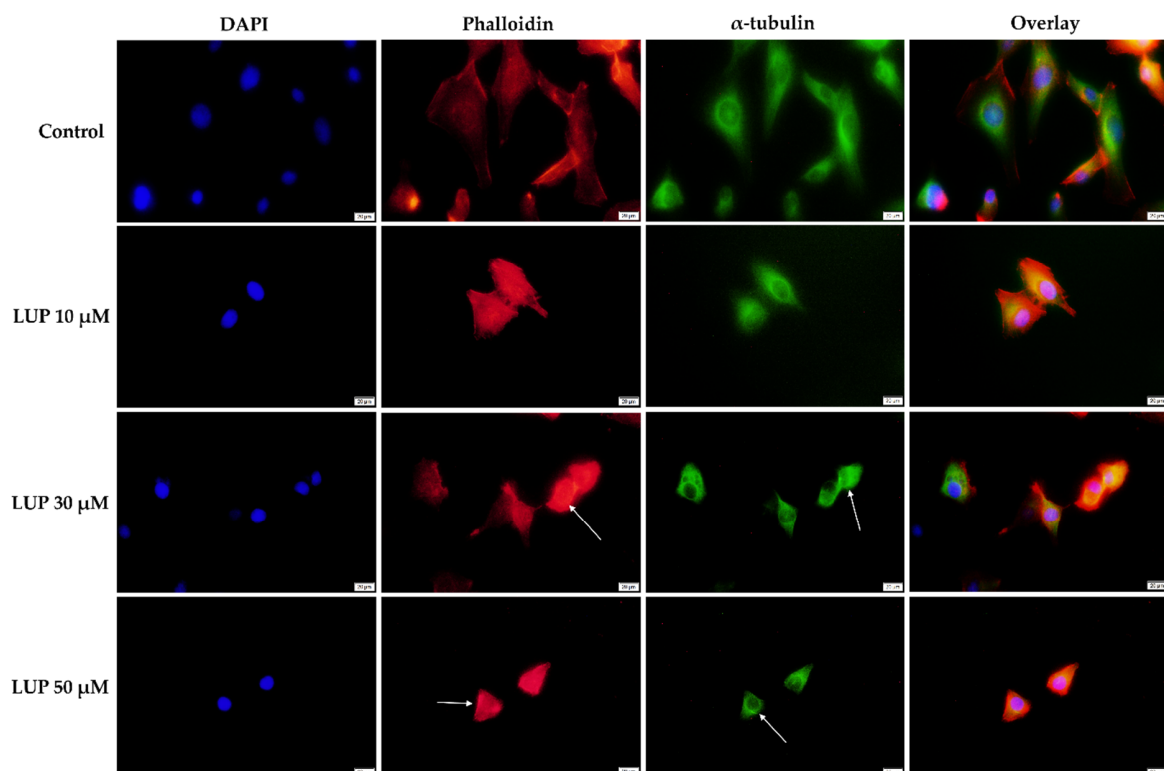


Figure 5. Human melanoma cells (RPMI-7951) visualized by fluorescence microscopy following the 24 h treatment with LUP (10, 30, and 50 μM). Cell nuclei (DAPI), actin filaments (phalloidin), and microtubules (α -tubulin) are presented individually and combined (overlay). The scale bars indicate 20 μm .

3.4. Wound Healing Assay

Taking into consideration that the high metastatic behavior is a fundamental characteristic of malignant melanoma cells, the potential anti-migratory property of LUP has been investigated by the means of a wound healing assay. For this assessment, the highest concentrations (40 and 50 μM) which caused significant cytotoxicity (Figure 1) in both cell lines were excluded. The effect exerted by LUP on A375 cells (Figure 6A) was highly dependent on the tested concentration. Therefore, at 10 μM (wound healing rate = 77.37%) a slight stimulation of the migratory capacity of cancer cells has been noticed as compared to control (wound healing rate = 71.55%). However, in contrast to this observation, LUP acted as a potent anti-migratory agent at 20 and 30 μM with recorded wound healing rates of 43.15% and 14.98%, respectively. In the case of RPMI-7951 cells (Figure 6B), an augmented effect has been noticed as compared to A375 cells. LUP inhibited the migration of the tumor cells at all concentrations in a dose-dependent manner, the most significant effect being recorded at 30 μM with a registered wound healing rate of 9.66%.

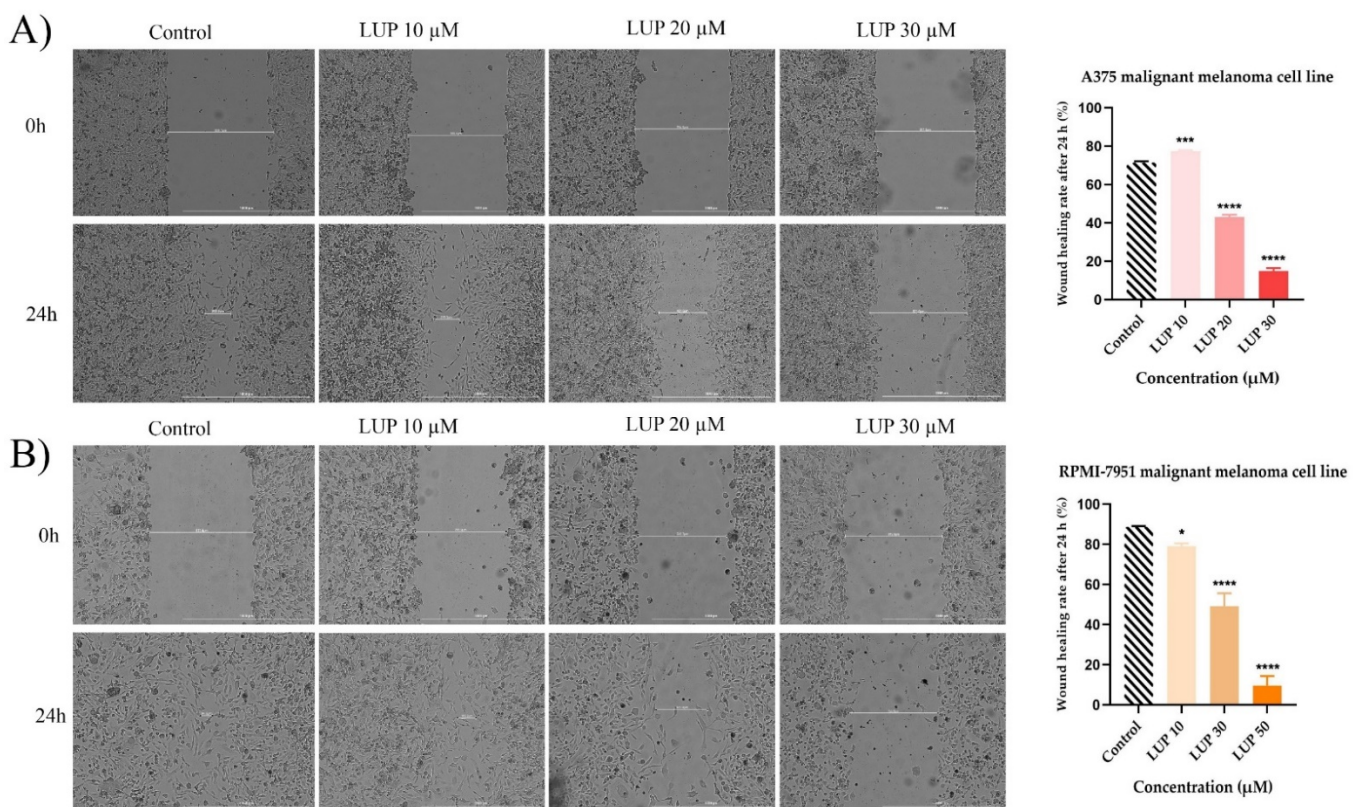


Figure 6. Representative images of the migratory capacity of (A) A375 and (B) RPMI-7951 MM cells following the treatment with LUP (10, 20, and 30 μM) for 24 h. The scale bars indicate 1000 μm . The bar graphs are presented as wound closure percentage after 24 h compared to the initial surface. The data are expressed as mean values \pm SD of three independent experiments performed in triplicate. The statistical differences between the control and the LUP-treated group were identified by applying the one-way ANOVA analysis followed by the Dunnett's multiple comparisons post-test (* $p < 0.1$; ** $p < 0.001$; *** $p < 0.0001$).

3.5. Chorioallantoic Membrane (CAM) Assay

To observe the effect of LUP on blood vessel development, the in ovo method was applied using the CAM assay. The potential antiangiogenic profile of LUP at the highest concentration tested in vitro (50 μM) was examined for 24 h. After this time interval, at the level of the vascular plexus, a series of changes were observed, such as the decrease in the capillary density, with certain areas at the level of the chorioallantoic membrane being devoid of vascularization. In addition, it is noteworthy that the blood vessels formed

are devoid of branches, this being a crucial aspect in terms of angiogenesis in the tumor process. Furthermore, at the level of the chorioallantoic membrane, a microhemorrhage can be observed, which after the treatment with LUP was prevented from evolving (Figure 7).

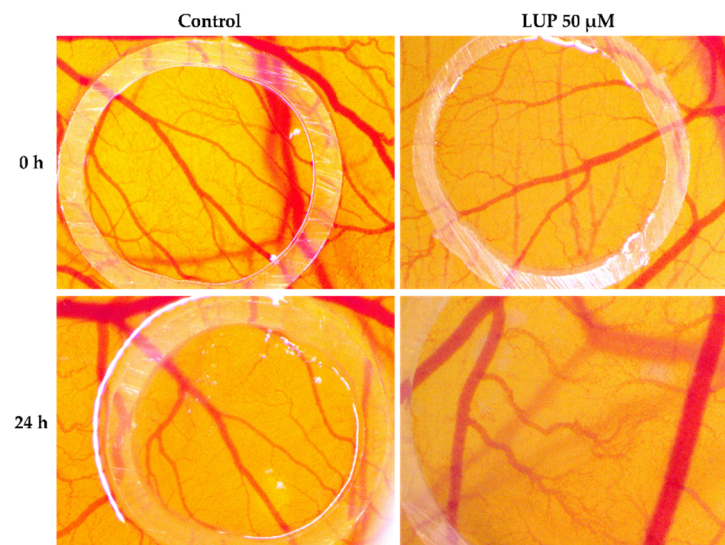


Figure 7. Stereomicroscopic imaging of the chorioallantoic membrane highlighting the angiogenic process after the treatment for 24 h with LUP 50 μ M.

4. Discussion

The present study aimed to explore whether LUP acts as a potent anti-cancer dietary compound that might be successfully included in malignant melanoma prophylaxis or chemotherapy, information that is rather inconclusive at present. Accordingly, an *in vitro* and *in ovo* investigation of the anti-proliferative, anti-migratory, and anti-angiogenic properties of LUP has been conducted using two MM cell lines—A375 and RPMI-7951. The main findings in this direction reveal that LUP exerts: (i) a dose-dependent and selective cytotoxicity against MM cells at micromolar concentrations (10–50 μ M) reflected by a decreased cell viability and confluence, apoptotic nuclear features, cytoskeletal alterations, cellular dysmorphology, and inhibited cell migration (Figures 1–6), as well as (ii) a potent anti-angiogenic effect (Figure 7).

LUP is a natural pentacyclic lupane-type triterpenoid [25] displaying a broad spectrum of pharmacological activities, including anti-inflammatory, anti-microbial, anti-diabetic, hepato-, nefro-, and cardio-protective properties which are detailed in an exhaustive review [26]. Furthermore, several studies direct the use of LUP towards the treatment of skin injuries. For instance, Beserra's research group shows that lupeol exerts beneficial effects in cutaneous repair both *in vitro* by promoting wound healing in human keratinocytes and fibroblasts, and *in vivo* by regulating collagen distribution and the expression of several markers (i.e., cytokines, NF- κ B, Ki-67, growth factor) [27,28]. Recent research focused on exploring the efficiency of LUP in the treatment of various cancers (i.e., lung, liver, pancreas, head, and neck), offering valuable insight into the molecular mechanisms underlying its anti-tumor properties [29–32]. With respect to the anti-melanoma effect of LUP, the scientific data remain insufficient. A previous study by Saleem et al. illustrated the ability of lupeol to decrease the viability of WM35 and 451 Lu melanoma cells in a concentration-dependent manner, induce G1-S phase cell cycle arrest, and initiate apoptosis after 72 h of treatment [33]. Similarly, another study by Tarapore and colleagues supports the anti-melanoma effect of LUP against MM cells (Mel 928, Mel 1241, and Mel 1011) by inducing apoptosis and specifically targeting the Wnt/b-catenin signaling after 48 h of treatment [34].

In the light of these previous discoveries, our research focused on gathering supplementary information regarding the anti-melanoma effect of LUP following a short-term

treatment (24 h). Our results indicate that LUP decreased the viability of A375 and RPMI-7951 human MM cells in a concentration-dependent trend (Figure 1A,B). The most notable cytotoxic activity has been recorded at the highest concentrations tested (40 and 50 μM), the cellular viability being reduced to 73.17% and 61.29% for A375, and 61.52% and 37.78% for RPMI-7951, respectively. The calculated IC_{50} values were $45.54 \pm 1.48 \mu\text{M}$ for RPMI-7951, and $66.59 \pm 2.20 \mu\text{M}$ for A375, suggesting a cell type-dependent intensity in the anti-melanoma effect of LUP which acted more potently against the RPMI-7951 cell line. As a consequence of the cellular death, a significant loss in cell confluence has been remarked in both cell lines at 30 and 50 μM (Figure 1C). Plant-derived compounds offer substantial benefits in cancer management due to their low toxicity when compared to classical chemotherapeutics [14]. However, toxicological screening is necessary during drug development to ensure the safety of the tested compound. Since *in vitro* studies represent an eligible platform for revealing the toxicity of substances [35], the viability assay has been performed on human keratinocytes (HaCaT) and fibroblasts (1BR3) as well. The obtained results indicate the absence of LUP-induced cytotoxicity in healthy skin cells in comparison to cancer cells. However, a slight reduction in their viability (to approximately 90%) has been noticed after 24 h of treatment with the highest concentration of LUP (50 μM)—Figure 2. The calculated IC_{50} values— $210.82 \pm 25.09 \mu\text{M}$ (HaCaT), and $346.25 \pm 12.84 \mu\text{M}$ (1BR3), are considerably higher than those estimated for A375 and RPMI-7951 MM cells, suggesting a selective anti-melanoma effect.

Apoptosis is a natural mechanism leading to programmed cell death. One of the hallmarks of cancer cells is their ability to evade apoptosis, a process that became a primary target in cancer therapy [36]. The changes generated in the A375 and RPMI-7951 cells' viability and confluence following the 24 h of treatment led to the implementation of the Hoechst 33342 staining to elucidate the potential cell death mechanism induced by LUP. Nuclear deformation has been observed at 30 and 50 μM in both cell lines, along with apoptosis-specific signs, such as fragmentation, chromatin condensation, membrane blebbing, and formation of apoptotic bodies (Figure 3).

The cytoskeleton is a network formed of intracellular filaments exerting important physiological functions in regard to cancer cell morphology, division, motility, and invasion [37]. During apoptosis, the cell cytoskeleton undergoes a dynamic rearrangement, leading to a change in cell morphology [38,39]. Several cytoskeletal and cell shape alternations have been recorded in A375 and RPMI-7951 MM cells following the 24 h treatment with LUP 30 and 50 μM (Figures 4 and 5), such as condensation of AF, reorganization of MTs into a cortical ring, cell rounding, and reduced longitudinal axis.

Taking into account the invasive nature of malignant melanoma cells, another aspect that has been researched in the present study is the impact of LUP on their migratory ability by performing a wound healing assay. Since at 40 and 50 μM signs of cytotoxicity were detected, the concentrations selected for this experiment were 10, 20 and 30 μM . LUP significantly inhibited the migration of RPMI-7951 cells at all concentrations as compared to the control, with wound healing rates of 79%, 49.21%, and 9.66%. Despite a slight stimulation observed at 10 μM , in A375 cells the results were similar to those obtained in RPMI-7951 cells, the registered wound healing rates being 43.15% and 14.98% at 20 and 30 μM , respectively. The data are presented in Figure 6.

Angiogenesis is a process of real importance in oncogenesis, given that malignant cells need oxygen and nutrients to grow, which are transported through blood vessels. Anti-angiogenic compounds have been developed to inhibit the formation of new blood vessels and also to block tumor growth [40–42]. Lupeol raises interest in terms of antiangiogenic effect, noting in the present study that after 24 h of treatment, LUP caused a considerable decrease in neovascularization, and at the chorioallantoic membrane level can be seen areas without vascularization (Figure 7). These results are supported by previous studies in order to highlight the antitumor and antiangiogenic effect of LUP. One such study is the one conducted by Avin et al. [43], in which the antiangiogenic effect of lupeol on the chorioallantoic membrane was similar to that observed in the present study. In addition,

by comparing the effect on blood vessels by lupeol and lectin, lupeol has been shown to be more effective due to its small molecular size [44].

5. Conclusions

The main objective of the present study was to conduct in vitro and in ovo investigations on the potential of lupeol in the treatment of malignant melanoma. The findings reveal an efficient and selective anti-melanoma effect exerted by LUP at μM concentrations (10–50) against A375 and RPMI-7951 MM cells characterized by: (i) a dose-dependent decrease in the cells' viability and confluence, (ii) apoptotic nuclear features, (iii) reorganization of the cytoskeletal components, and (iv) inhibition of the cells' migratory ability. Furthermore, our study suggests that LUP is able to reduce the formation of neovascularization and thus inhibit angiogenesis, being a potential antiangiogenic agent useful in antitumor therapy. Further studies are required for elucidating the mechanisms of LUP-induced in vitro anti-cancer and in ovo anti-angiogenic effects.

Author Contributions: Conceptualization, C.A.D.; data curation, F.B. and C.P.; formal analysis, A.M.; funding acquisition, I.P.; investigation, I.M. and S.A.; methodology, I.G.M. and S.A.; resources, I.P. and C.A.D.; software, C.P.; supervision, C.A.D.; validation, C.G.; visualization, C.G.; writing—original draft, F.B., I.G.M. and I.M.; writing—review and editing, A.M. and C.A.D. All authors have read and agreed to the published version of the manuscript.

Funding: This research was partially funded by the Romanian Ministry of Education and Research, the National Council for the Financing of Higher Education, grant number CNFIS-FDI-2021-0498.

Institutional Review Board Statement: Not applicable.

Informed Consent Statement: Not applicable.

Data Availability Statement: The data presented in this study are available on request from the corresponding author.

Conflicts of Interest: The authors declare no conflict of interest.

References

1. Jenkins, R.W.; Fisher, D.E. Treatment of Advanced Melanoma in 2020 and Beyond. *J. Investig. Dermatol.* **2021**, *141*, 23–31. [[CrossRef](#)] [[PubMed](#)]
2. Burns, D.; George, J.; Aucoin, D.; Bower, J.; Burrell, S.; Gilbert, R.; Bower, N. The Pathogenesis and Clinical Management of Cutaneous Melanoma: An Evidence-Based Review. *J. Med. Imaging Radiat. Sci.* **2019**, *50*, 460–469.e1. [[CrossRef](#)]
3. Naik, P.P. Cutaneous Malignant Melanoma: A Review of Early Diagnosis and Management. *World J. Oncol.* **2021**, *12*, 7–19. [[CrossRef](#)]
4. Gordon, R. Skin cancer: An overview of epidemiology and risk factors. *Semin. Oncol. Nurs.* **2013**, *29*, 160–169. [[CrossRef](#)]
5. Carr, S.; Smith, C.; Wernberg, J. Epidemiology and Risk Factors of Melanoma. *Surg. Clin. N. Am.* **2020**, *100*, 1–12. [[CrossRef](#)]
6. Domingues, B.; Lopes, J.; Soares, P.; Populo, H. Melanoma treatment in review. *Immuno Targets Ther.* **2018**, *7*, 35–49. [[CrossRef](#)] [[PubMed](#)]
7. de Oliveira Júnior, R.G.; Ferraz, C.A.A.; e Silva, M.G.; de Lavor, É.M.; Rolim, L.A.; de Lima, J.T.; Fleury, A.; Picot, L.; de Souza Siqueira Quintans, J.; Quintans Júnior, L.J.; et al. Flavonoids: Promising Natural Products for Treatment of Skin Cancer (Melanoma). In *Natural Products and Cancer Drug Discovery*; Badria, F.A., Ed.; IntechOpen: Rijeka, Croatia, 2017. Available online: <https://www.intechopen.com/chapters/54517> (accessed on 24 September 2021). [[CrossRef](#)]
8. Luke, J.J.; Schwartz, G.K. Chemotherapy in the Management of Advanced Cutaneous Malignant Melanoma. *Clin. Dermatol.* **2013**, *31*, 290–297. [[CrossRef](#)] [[PubMed](#)]
9. Chinembiri, T.N.; Du Plessis, L.H.; Gerber, M.; Hamman, J.H.; Du Plessis, J. Review of natural compounds for potential skin cancer treatment. *Molecules* **2014**, *19*, 11679–11721. [[CrossRef](#)]
10. Ijaz, S.; Akhtar, N.; Khan, M.S.; Hameed, A.; Irfan, M.; Arshad, M.A.; Ali, S.; Asrar, M. Plant derived anticancer agents: A green approach towards skin cancers. *Biomed. Pharmacother.* **2018**, *103*, 1643–1651. [[CrossRef](#)]
11. Kim, T.; Amaria, R.N.; Spencer, C.; Reuben, A.; Cooper, Z.A.; Wargo, J.A. Combining targeted therapy and immune checkpoint inhibitors in the treatment of metastatic melanoma. *Cancer Biol. Med.* **2014**, *11*, 237–246. [[CrossRef](#)] [[PubMed](#)]
12. Akaike, T.; Nghiem, P.; Lacouture, M.E. CME Part I: Immune checkpoint inhibitors to treat cutaneous malignancies. *J. Am. Acad. Dermatol.* **2020**, *83*, 1239–1253. [[CrossRef](#)]
13. Majolo, F.; de Oliveira Becker Delwing, L.K.; Marmitt, D.J.; Bustamante-Filho, I.C.; Goettert, M.I. Medicinal plants and bioactive natural compounds for cancer treatment: Important advances for drug discovery. *Phytochem. Lett.* **2019**, *31*, 196–207. [[CrossRef](#)]

14. Dehelean, C.A.; Marcovici, I.; Soica, C.; Mioc, M.; Coricovac, D.; Iurciuc, S.; Cretu, O.M.; Pinzaru, I. Plant-Derived Anticancer Compounds as New Perspectives in Drug Discovery and Alternative Therapy. *Molecules* **2021**, *26*, 1109. [CrossRef]
15. Sarek, J.; Kvasnica, M.; Vlk, M.; Urban, M.; Dzubak, P.; Hajdich, M. The Potential of Triterpenoids in the Treatment of Melanoma. In *Research on Melanoma—A Glimpse into Current Directions and Future Trends*; Murph, M., Ed.; IntechOpen: Rijeka, Croatia, 2011. Available online: <https://www.intechopen.com/chapters/19095> (accessed on 6 September 2021). [CrossRef]
16. Liu, K.; Zhang, X.; Xie, L.; Deng, M.; Chen, H.; Song, J.; Long, J.; Li, X.; Luo, J. Lupeol and its derivatives as anticancer and anti-inflammatory agents: Molecular mechanisms and therapeutic efficacy. *Pharmacol. Res.* **2021**, *164*, 105373. [CrossRef]
17. Saleem, M. Lupeol, a novel anti-inflammatory and anti-cancer dietary triterpene. *Cancer Lett.* **2009**, *285*, 109–115. [CrossRef] [PubMed]
18. Shen, X.; Cui, X.; Cui, H.; Jin, Y.; Jin, W.; Sun, H. Geraniol and lupeol inhibit growth and promote apoptosis in human hepatocarcinoma cells through the MAPK signaling pathway. *J. Cell. Biochem.* **2019**, *120*, 5033–5041. [CrossRef] [PubMed]
19. Wang, Y.; Hong, D.; Qian, Y.; Tu, X.; Wang, K.; Yang, X.; Shao, S.; Kong, X.; Lou, Z.; Jin, L. Lupeol inhibits growth and migration in two human colorectal cancer cell lines by suppression of wnt- β -catenin pathway. *Onco Targets Ther.* **2018**, *11*, 7987–7999. [CrossRef]
20. Min, T.R.; Park, H.J.; Ha, K.T.; Chi, G.Y.; Choi, Y.H.; Park, S.H. Suppression of EGFR/STAT3 activity by lupeol contributes to the induction of the apoptosis of human non-small cell lung cancer cells. *Int. J. Oncol.* **2019**, *55*, 320–330. [CrossRef] [PubMed]
21. Felice, F.; Zambito, Y.; Belardinelli, E.; Fabiano, A.; Santoni, T.; Di Stefano, R. Effect of different chitosan derivatives on in vitro scratch wound assay: A comparative study. *Int. J. Biol. Macromol.* **2015**, *76*, 236–241. [CrossRef] [PubMed]
22. Simu, S.; Marcovici, I.; Dobrescu, A.; Malita, D.; Dehelean, C.A.; Coricovac, D.; Olaru, F.; Draghici, G.A.; Navolan, D. Insights into the behavior of triple-negative mda-mb-231 breast carcinoma cells following the treatment with 17 β -ethinylestradiol and levonorgestrel. *Molecules* **2021**, *26*, 2776. [CrossRef] [PubMed]
23. Nowak-Sliwinska, P.; Segura, T.; Iruela-Arispe, M.L. The chicken chorioallantoic membrane model in biology, medicine and bioengineering. *Angiogenesis* **2014**, *17*, 779–804. [CrossRef]
24. Crowley, L.C.; Marfell, B.J.; Waterhouse, N.J. Analyzing cell death by nuclear staining with Hoechst 33342. *Cold Spring Harb. Protoc.* **2016**, *2016*, 778–781. [CrossRef]
25. Tsai, F.S.; Lin, L.W.; Wu, C.R. Lupeol and Its Role in Chronic Diseases. *Adv. Exp. Med. Biol.* **2016**, *929*, 145–175. [CrossRef]
26. Siddique, H.R.; Saleem, M. Beneficial health effects of lupeol triterpene: A review of preclinical studies. *Life Sci.* **2011**, *88*, 285–293. [CrossRef] [PubMed]
27. Beserra, F.P.; Xue, M.; De Azevedo Maia, G.L.; Rozza, A.L.; Pellizzon, C.H.; Jackson, C.J. Lupeol, a pentacyclic triterpene, promotes migration, wound closure, and contractile effect in vitro: Possible involvement of PI3K/Akt and p38/ERK/MAPK pathways. *Molecules* **2018**, *23*, 2819. [CrossRef]
28. Beserra, F.P.; Gushiken, L.F.S.; Vieira, A.J.; Bérغامo, D.A.; Bérغامo, P.L.; de Souza, M.O.; Hussni, C.A.; Takahira, R.K.; Nóbrega, R.H.; Martinez, E.R.M.; et al. From inflammation to cutaneous repair: Topical application of lupeol improves skin wound healing in rats by modulating the cytokine levels, NF- κ B, Ki-67, growth factor expression, and distribution of collagen fibers. *Int. J. Mol. Sci.* **2020**, *21*, 4952. [CrossRef]
29. Babu, T.S.; Michael, B.P.; Jerard, C.; Vijayakumar, N.; Ramachandran, R. Study on the anti metastatic and anti cancer activity of triterpene compound lupeol in human lung cancer. *Int. J. Pharm. Sci. Res.* **2019**, *10*, 721–727. [CrossRef]
30. Bhattacharyya, S.; Sekar, V.; Majumder, B.; Mehrotra, D.G.; Banerjee, S.; Bhowmick, A.K.; Alam, N.; Mandal, G.K.; Biswas, J.; Majumder, P.K.; et al. CDKN2A-p53 mediated antitumor effect of Lupeol in head and neck cancer. *Cell. Oncol.* **2017**, *40*, 145–155. [CrossRef]
31. Eldohaji, L.M.; Fayed, B.; Hamoda, A.M.; Ershaid, M.; Abdin, S.; Alhamidi, T.B.; Mohammad, M.G.; Omar, H.A.; Soliman, S.S.M. Potential targeting of Hep3B liver cancer cells by lupeol isolated from *Avicennia marina*. *Arch. Pharm.* **2021**, *354*, e2100120. [CrossRef] [PubMed]
32. Saleem, M.; Murtaza, I.; Tarapore, R.S.; Suh, Y.; Adhami, V.M.; Johnson, J.J.; Siddiqui, I.A.; Khan, N.; Asim, M.; Hafeez, B.; et al. Lupeol inhibits proliferation of human prostate cancer cells by targeting β -catenin signaling. *Carcinogenesis* **2009**, *30*, 808–817. [CrossRef]
33. Saleem, M.; Maddodi, N.; Zaid, M.A.; Khan, N.; Bin Hafeez, B.; Asim, M.; Suh, Y.; Yun, J.M.; Setaluri, V.; Mukhtar, H. Lupeol inhibits growth of highly aggressive human metastatic melanoma cells in vitro and in vivo by inducing apoptosis. *Clin. Cancer Res.* **2008**, *14*, 2119–2127. [CrossRef] [PubMed]
34. Tarapore, R.S.; Siddiqui, I.A.; Saleem, M.; Adhami, V.M.; Spiegelman, V.S.; Mukhtar, H. Specific targeting of wnt/ β -catenin signaling in human melanoma cells by a dietary triterpene lupeol. *Carcinogenesis* **2010**, *31*, 1844–1853. [CrossRef]
35. Parasuraman, S. Toxicological screening. *J. Pharmacol. Pharmacother.* **2011**, *2*, 74–79. [CrossRef]
36. Pfeffer, C.M.; Singh, A.T.K. Apoptosis: A target for anticancer therapy. *Int. J. Mol. Sci.* **2018**, *19*, 448. [CrossRef]
37. Zhang, X.; Pei, Z.; Ji, C.; Zhang, X.; Xu, J.; Wang, J. Novel Insights into the Role of the Cytoskeleton in Cancer. In *Cytoskeleton—Structure, Dynamics, Function and Disease*; Jimenez-Lopez, J.C., Ed.; IntechOpen: Rijeka, Croatia, 2017. Available online: <https://www.intechopen.com/chapters/53708> (accessed on 28 August 2021). [CrossRef]
38. Povea-Cabello, S.; Oropesa-Ávila, M.; de la Cruz-Ojeda, P.; Villanueva-Paz, M.; De La Mata, M.; Suárez-Rivero, J.M.; Álvarez-Córdoba, M.; Villalón-García, I.; Cotán, D.; Ybot-González, P.; et al. Dynamic reorganization of the cytoskeleton during apoptosis: The two coffins hypothesis. *Int. J. Mol. Sci.* **2017**, *18*, 2393. [CrossRef] [PubMed]

39. Oropesa-Ávila, M.; de la Cruz-Ojeda, P.; Porcuna, J.; Villanueva-Paz, M.; Fernández-Vega, A.; de la Mata, M.; de Laverá, I.; Rivero, J.M.S.; Luzón-Hidalgo, R.; Álvarez-Córdoba, M.; et al. Two coffins and a funeral: Early or late caspase activation determines two types of apoptosis induced by DNA damaging agents. *Apoptosis* **2017**, *22*, 421–436. [[CrossRef](#)] [[PubMed](#)]
40. Lugano, R.; Ramachandran, M.; Dimberg, A. Tumor angiogenesis: Causes, consequences, challenges and opportunities. *Cell. Mol. Life Sci.* **2020**, *77*, 1745–1770. [[CrossRef](#)] [[PubMed](#)]
41. Mioc, M.; Avram, S.; Bercean, V.; Porcarasu, M.B.; Soica, C.; Susan, R.; Kurunczi, L. Synthesis, Characterization and Antiproliferative Activity Assessment of a Novel 1H-5-mercapto-1,2,4 Triazole Derivative. *Rev. Chim.* **2017**, *68*, 745–747. [[CrossRef](#)]
42. Lopes-Coelho, F.; Martins, F.; Pereira, S.A.; Serpa, J. Anti-angiogenic therapy: Current challenges and future perspectives. *Int. J. Mol. Sci.* **2021**, *22*, 3765. [[CrossRef](#)]
43. Vijay Avin, B.R.; Prabhu, T.R.C. New role of lupeol in reticence of angiogenesis, the cellular parameter of neoplastic progression in tumorigenesis models through altered gene expression. *Biochem. Biophys. Res. Commun.* **2014**, *448*, 139–144. [[CrossRef](#)]
44. Ambasta, R.K.; Jha, S.K.; Kumar, D.; Sharma, R.; Jha, N.K.; Kumar, P. Comparative study of anti-angiogenic activities of luteolin, lectin and lupeol biomolecules. *J. Transl. Med.* **2015**, *13*, 307. [[CrossRef](#)] [[PubMed](#)]